HEAT TRANSFER FROM TWO DISCRETE FLUSH-MOUNTED HEATERS SUBJECTED TO LAMINAR PULSATING AIR FLOW IN A CHANNEL

Unal Akdag
Department of Mechanical Engineering, Aksaray University, TR-68100, Aksaray, Turkey
E-mail: uakdag@gmail.com

Received January 2012, Accepted November 2012
No. 12-CSME-07, E.I.C. Accession 3328

ABSTRACT

In this article, a numerical study on heat transfer in laminar pulsating air flow in a channel around two discrete flush-mounted heat sources is reported. Simulations are conducted for five different frequencies and three different amplitudes while the Reynolds number ($Re = 125$) and Prandtl number ($Pr = 0.71$) remain constant for all cases. In addition, limited geometric parameters such as spacing between the two discrete heaters are investigated. Numerical simulations are performed by using the commercial CFD code Fluent. The optimum heat transfer parameters are analyzed. The time-mean Nusselt number is obtained for a cycle and given as dimensionless parameters. The heat transfer enhancements are found for low frequencies and high amplitudes.

Keywords: pulsating flow; discrete heaters; heat transfer enhancement; CFD.

TRANSFERT D'ÉNERGIE THERMIQUE DE DEUX SOURCES DE CHALEUR ENCASTRÉES EN ÉCOULEMENT D'AIR LAMINAIRE ET PULSATOIRE DANS UNE CONDUITE

RÉSUMÉ

Dans cet exposé, nous faisons état d'une étude numérique sur le transfert thermique en écoulement d'air laminaire et pulsatoire en canal autour de deux sources de chaleur encastrées. On a procédé à des simulations pour cinq différentes fréquences et trois différentes amplitudes, alors que les nombres de Reynolds ($Re = 125$) et Prandtl ($Pr = 0.71$) demeurent constants dans tous les cas. De plus, des paramètres géométriques limités, tels que l'espace entre les deux sources de chaleur, sont étudiés. Des simulations numériques sont effectuées en utilisant le code CFD Fluent. Les paramètres de transfert thermique sont analysés. La moyenne temporelle du nombre de Nusselt est obtenue pour un cycle. L'amélioration du transfert thermique est observée pour les basses fréquences et les hautes amplitudes.

Mots-clés : flux par pulsion ; éléments de chauffage discontinu ; amélioration du transfert d'énergie ; CFD.

NOMENCLATURE

A	area (m^2)
A_0	dimensionless amplitude [$A_0 = x_m/H$]
b	half the channel heigh (m)
g	gravity (m/s^2)
$h(x,t)$	local heat transfer coefficient (W/m^2-K)
h_p	average heat transfer coefficient for pulsating flow (W/m^2-K)
H	channel heigh-characteristic length [$2b = H$] (m)
k	conductivity (W/m−K)
L	total channel length (m)
l	heater length (m)
Nu_x	local instantaneous Nusselt number
Nu_p	average (time-mean) Nusselt number for pulsating flow
Nu_s	average Nusselt number for steady flow
P	pressure (N/m^2)
Pr	Prandtl number [$Pr = \upsilon/\alpha$]
q''	heat flux from heater surface (W/m^2)
Re	Reynolds number [$Re = U_o H/\upsilon$]
t	time (s)
T	temperature (K)
T_b	instant bulk temperature
$\overline{T}_b$	time-mean bulk temperature
T_w	instant average heater surface temperature
$\overline{T}_w$	time-mean heater temperature
u	instantaneous velocity (m/s)
u_s	steady component of velocity
u_t	pulsating component of velocity
U_0	average inlet velocity
Wo	Womersley number [$Wo = b\sqrt{\omega/\upsilon}$]
w	distance between two heaters (m)
x_m	amplitude (m)
x,y	cartesian coordinates
Greek symbols	
τ	cycle time [$\tau = \omega t$]
ρ	fluid density (kg/m^3)
ω	angular frequency (rad/s)
υ	kinematic viscosity (m/s^2)
Subscripts	
b	bulk
w	wall

1. INTRODUCTION

Nowadays, cooling requirements are significantly increasing due to the miniaturization of electronic equipments. The effective cooling of heat-generated components is becoming the most important research topic, because of the increasing heat generation rate and increasing component density. The commonly used methods for the cooling of electronic equipments are free and forced convection. However, these methods are not sufficiently unaccompanied for the effective cooling of components; even so, the strong forced convection is not allowed in some applications. New techniques are required for the cooling of devices in a

more effective, reliable and economic manner [1–4]. Especially, for the cooling of miniaturized electronic devices operating in narrow areas, more sophisticated cooling methods have consistently received much attention in recent years. The alternative cooling methods are becoming the current research topics, and one of the most promising methods is the cooling by pulsating flow [5,6].

The pulsating flow includes the steady and time-dependent velocity component [7]. Typical and natural examples of pulsating flows are the arterial flows in the human body. Pulsating flow and heat transfer occur in many industrial applications, such as pulse combustor, pulse tube cry-cooler, cooling system of nuclear reactor, pulse-jet and compressors, electronic cooling, and so on. The pulsating flow parameters affect the performance of many thermal engineering applications. When pulsations are applied to the flow, then a change in heat transfer to or from it can be expected, because the pulsation would change the thickness of the boundary layer and thus the thermal resistance. From this perspective, an increase in the heat transfer due to the decreasing of the boundary layer thickness is expected [8]. Therefore, recently, great interest is being evinced in studying the effects of pulsating flow on convective heat transfer.

Many researchers have presented experimental, numerical and analytical studies on the effect of pulsation on heat transfer characteristics. Experimental investigations on laminar pulsating flow have been performed by researchers [9–16]. Among these studies, the characteristics of laminar pulsating flow within a tube or channel under uniform constant heat flux have been experimentally investigated by Habib et al. [9]. An increase as well as a reduction in Nusselt number has been reported, depending on both Reynolds number and frequency. Kearney et al. [13] experimentally investigated the time-resolved structure of a thermal boundary layer in a laminar pulsating channel flow. They reported that differing degrees of flow reversal showed that the primary impact of reversed flow is an increase in the instantaneous thermal boundary layer thickness and a period of decreased instantaneous Nusselt number. They concluded that flow reversal is not necessarily a requirement for enhancement. An experimental study for forced convection heat transfer in laminar pulsating flow inside a tube was studied by Mostafa et al. [14]. The amount of heat transfer declines in the case of laminar flow, compared with steady flow. Flow pulsation reportedly causes a decrease in Nusselt number, about 22 % of the average value than the steady flow. Zohir et al. [15] investigated the heat transfer characteristic inside a pipe for a wide range of Reynolds numbers. They defined the range of improvement of heat transfer coefficient with pulsating flow for both laminar and turbulent flow regimes. Mamayev et al. [16] found that, at low frequencies the heat transfer rate for pulsed air flow is lower than that of the steady flow. As frequency increased, the relative heat transfer coefficient also increased.

Due to the complicated nature of the analytical solution, only a limited number of studies are available on heat transfer in pulsating laminar flow [17–23]. A remarkable analytical study was performed on the laminar pulsating pipe flow by Faghri et al. [18], who reported that higher heat transfer rates were produced at high frequencies, and that the Nusselt number increases proportionally to the pulsation frequency. Recently, Nield and Kuznetsov [23], obtained analytical expressions for velocity, temperature distribution, and transient Nusselt number for the problem of forced convection, in a parallel-plate channel or a circular tube using the perturbation method. The Nusselt number gradually increases with a decrease in the Prandtl number.

Heat transfer in a pulsating laminar flow was also numerically studied and a variety of contradictory results were reported [24–30]. They have observed that at the fully established downstream region, the Nusselt number may increase or decrease according to frequency parameters. Although some investigators reported conflicting results, in recently common views on this issue, the pulsating effect contributes to heat transfer enhancement [27]. As understood from literature just mentioned, it is important to choose appropriate pulsating flow parameters for improving heat transfer. To ascertain this, new studies are required to clarify the physical phenomena of pulsating flow. Detailed experimental and numerical investigations can reveal the key characteristics of designing of new pulse-type heat transfer devices for various specifications.

The fundamental problem of how to allocate discrete heat sources to the space on a wall cooled by forced convection is investigated in literature. Several papers have been published on the heat transfer performance of walls with distributed heat sources [31–35]. Some have recognized the opportunity to improve global performance by optimizing the non-uniform distribution of discrete heat sources [36,37]. Despite the large amount of research on forced convection heat transfer in a discretely heated channel, a comprehensive study has not been performed on the discrete heaters subjected to pulsating flow. In this context, the present article aims at extending our understanding of the physical phenomena present for two discrete heaters that are cooled by pulsating flow.

In this article, a numerical study on heat transfer in a pulsating laminar air flow within a channel around two discrete heaters over a wide range of Womersley number and large fluid amplitudes with a simple geometric parameter is reported. Numerical calculations are performed by using Fluent CFD package. Detailed numerical results are obtained to describe the effects of externally controllable parameters such as pulsation frequency and amplitude. To explain the heat transfer mechanism, instantaneous velocity and temperature profiles are obtained. The instantaneous bulk and wall temperatures are considered over a cycle to calculate the average temperatures. The time-mean Nusselt number for per cycle is obtained and given as dimensionless parameters. This geometry is of particular interest in the cooling of electronic systems and in the design of heat exchanger and other thermal systems.

2. PROBLEM DEFINITION

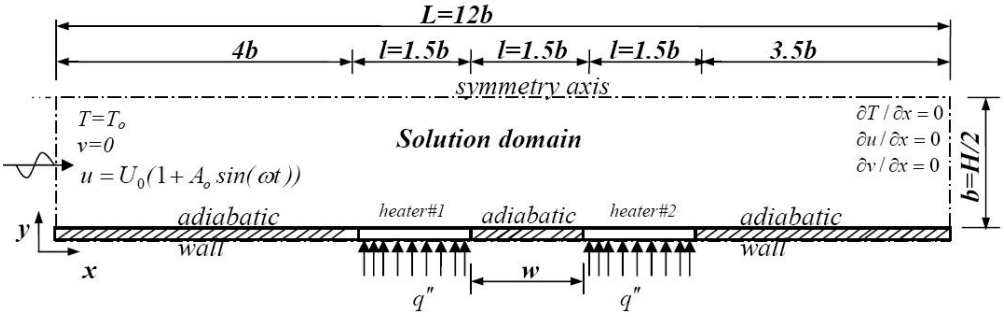

Fig. 1. Schematic view of flow domain and dimensions.

The geometry to be studied is a 2d channel, as represented in Fig. 1, with the corresponding boundary conditions, where the channel size is fixed at $H \times L = 20 \times 120$ mm initially. Then, the distance between two discrete heaters is changed for investigation of the effect on the heat transfer. It is a plane duct with two discrete heaters located at the channel wall. From heaters the condition of constant heat flux ($q'' = 400$ W/m^2) is imposed. The fluid inlets to the channel have a pulsating component and a uniform temperature ($T_o = 300$ K). The thermal properties of the fluid are assumed to be constant and viscous dissipations are assumed negligible. Due to the symmetry, only half the channel is considered a solution domain. Air is the working fluid, and is assumed to be incompressible.

3. MATHEMATICAL FORMULATION

3.1. Governing Equations

The velocity field of a pulsating fluid flow in a 2d channel (with large enough width) can be expressed by:

$$u(y,t) = u_s(y) + u_t(y,t)\,, \tag{1}$$

where $u_s(y)$ is the steady flow velocity, whereas $u_t(y,t)$ is the imposed unsteady velocity component. The governing equations for laminar, incompressible, time-dependent velocity and temperature field in a 2d channel can be expressed as follows, based on the assumptions of constant properties and negligible viscous dissipation:

$$\frac{\partial u}{\partial x}+\frac{\partial v}{\partial y}=0\,, \tag{2}$$

$$\frac{\partial u}{\partial t}+u\frac{\partial u}{\partial x}+v\frac{\partial u}{\partial y}=-\frac{1}{\rho}\frac{\partial p}{\partial x}+\upsilon\left(\frac{\partial^2 u}{\partial x^2}+\frac{\partial^2 u}{\partial y^2}\right), \tag{3}$$

$$\frac{\partial v}{\partial t}+u\frac{\partial v}{\partial x}+v\frac{\partial v}{\partial y}=-\frac{1}{\rho}\frac{\partial p}{\partial y}+\upsilon\left(\frac{\partial^2 v}{\partial x^2}+\frac{\partial^2 v}{\partial y^2}\right), \tag{4}$$

$$\frac{\partial T}{\partial t}+u\frac{\partial T}{\partial x}+v\frac{\partial T}{\partial y}=\alpha\left(\frac{\partial^2 T}{\partial x^2}+\frac{\partial^2 T}{\partial y^2}\right), \tag{5}$$

where u and v represent the x and y velocity components, respectively. The temperature is denoted by T, and dynamic pressure is denoted by p. The thermal diffusivity is denoted by $\alpha = k/\rho c_p$, where ρ, c_p, k and ν are the density, specific heat, thermal conductivity and kinematic viscosity of the fluid, respectively.

3.2. Boundary Conditions

The "velocity inlet" boundary conditions are utilized at the channel inlet, using the Fluent software. The inlet velocity includes a pulsating component with time-varying sinusoidal and is defined as follows:

$$u = U_0\left[1+A_0\sin(\omega t)\right], \tag{6}$$

where U_0 is the average inlet velocity at $x=0$, and A_0 is the oscillating amplitude of the inlet velocity. This velocity is defined into the Fluent utilizing a user-defined function. The outflow boundary condition is applied to the channel exit. Symmetry boundary conditions have been applied to the middle of the channel heights of the model due to the symmetry. The constant heat flux boundary condition is applied to the heater surfaces. For the other surfaces, adiabatic wall boundary conditions have been applied as illustrated in Fig. 1. No-slip boundary conditions are applied to all solid boundaries. These associated boundary conditions are described as follow mathematically:

- At the channel walls, at $y=0$, for $0<x<4b$, $5.5b<x<7b$, $8.5b<x<12b$:

$$u(x,0,t)=0\,, \tag{7a}$$

$$v(x,0,t)=0\,, \tag{7b}$$

$$\frac{\partial T}{\partial y}(x,0,t)=0\,. \tag{7c}$$

- For discrete heaters, $4b<x<5.5b$, $7b<x<8.5b$:

$$u(x,0,t)=0\,, \tag{7d}$$

$$v(x,0,t)=0\,, \tag{7e}$$

$$-k\frac{\partial T}{\partial y}(x,0,t)=q''\,. \tag{7f}$$

- At the channel centerline for symmetry, at $y = b$:

$$\frac{\partial u}{\partial x}(x,b,t) = 0\,, \tag{7g}$$

$$\frac{\partial v}{\partial x}(x,b,t) = 0\,, \tag{7h}$$

$$\frac{\partial T}{\partial x}(x,b,t) = 0\,. \tag{7i}$$

At the channel exit, the flow is assumed to have attained fully developed conditions. Figure.1 illustrated this state. It is relevant to note that this assumption of negligible gradients of velocity and temperature at the outlet that is because for pulsating flow the fully developed conditions is usually shorter than the uniform flow. The periodic flow or pulsating flow may not have sufficient run to become fully developed in each section of channel [7,29,38]. It should be noted that the inlet and outlet conditions will be changed at the each half-cycle because of the flow reversal.

3.3. Physical Parameters

The following non dimensional quantities are used for presenting the results. These quantities are Reynolds number, $Re = U_0 H \big/ \upsilon$; Womersley number, $Wo = b\sqrt{\omega/\upsilon}$; dimensionless amplitude, $A_o = x_m \big/ H$; and geometric parameter; w/H, respectively. Where, H is the channel height (characteristic length), and υ is the kinematic viscosity of the fluid. In addition, ω is the angular frequency, and w is the distance between heaters. Despite the Prandtl number (Pr) and other geometric parameters are affecting the physics of flow, which remains constant for all cases in this study.

4. NUMERICAL SOLUTION

Due to the symmetry, only one half of the channel is modeled. The model is created and meshed using the Gambit software. In this study, the governing flow and energy equations subjected to the aforementioned boundary conditions are numerically solved using the commercial code Fluent 6.1.22. The momentum equations are discretized using a second-order upwind discretization scheme. The pressure term is first discretized using the second-order scheme, and then, both the pressure and the velocity terms are coupled with each other employing the Pressure-Implicit with Splitting of Operators (PISO) scheme. The unsteady segregated solver is used with the second-order upwind scheme or convective terms in the mass, momentum and energy equations for laminar, 2d flows. The convergence criterion is set at 10^{-3} for mass and momentum equations, whereas the energy equation is set at 10^{-6}.

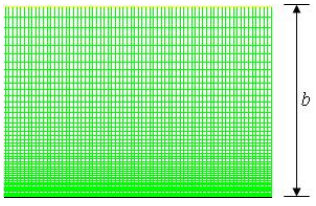

Fig. 2. Typical grid structure for present study.

Evaluating the grid-independent solutions is also an important aspect for minimizing the error in CFD results. Therefore, it is practical to achieve the grid-independent solutions using several tests on a computational mesh. The computational domain, which consists of a mesh layout with approximately 30,000 cells,

is presented in Fig. 2. The grid is highly concentrated near the wall to analyze the boundary layer interactions. For grid independence, the number of cells varied from 15,000 to 45,000 in various steps. After 30,000 cells, a further increase in cells was found to have less than 2 % variation in Nusselt number, which is taken as the criterion for grid independence. Numerical solution parameters are given in Table 1.

Frequency, Wo	Amplitude, A_0			Geometry, w/H
	$A_0 = 1$	$A_0 = 2.5$	$A_0 = 5$	
7	Case-1	Case-6	Case-11	0.75
14	Case-2	Case-7	Case-12	0.75
≅ 20	Case-3	Case-8	Case-13	0.75
≅ 29	Case-4	Case-9	Case-14	0.75
≅ 44	Case-5	Case-10	Case-15	0.75
14	-	-	Case-16	0.375
14	-	-	Case-17	1.15
14	-	-	Case-18	1.5

Table 1. Numerical simulation parameters.

4.1. Verification of Solutions

In order to verify the accuracy of the present numerical study, the present numerical procedure was compared with the experimental results of Incropera et al. [33]. They investigated convective heat transfer from a single and an array of flush mounted discrete heaters for water in a rectangular channel. They were using the single heater length to calculate the Nusselt number for laminar regime. For comparison similar definition is used. Despite the working fluid discrepancy between present study and [33], created the similar conditions for comparison. In accordance with the appropriate parameters of [33], the Reynolds number was set at $Re = 1000$. For single heater, the deviation of the numerical results of the present study is less than 5 % compared to the experimental values of Incropera et al. [33].

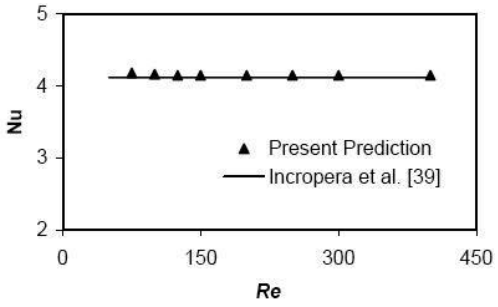

Fig. 3. Verification of Nu number with open literature [39].

In addition, to give credence to the accuracy and reliability of the present numerical solutions, due to the absence of similar flow conditions for heat transfer to pulsating flow in the literature the verification of the heat transfer (Nusselt number) is performed by comparing against the laminar steady channel flow as shown in Fig. 3. The present numerical smooth channel result is found to be in excellent agreement with the exact solution values obtained from the open literature [39] for Nusselt number less than ±2 % deviation. This provides a strong confidence in further investigation of the pulsating channel flow.

5. RESULTS AND DISCUSSIONS

In this section, the heat transfer mechanism is discussed using the pulsating laminar flow in a channel by examining the effects of various parameters. The Reynolds number ($Re = 125$), Prandtl number ($Pr = 0.71$) and geometric parameters are kept constant (except w/H) for all cases. The changed parameters for numerical calculations are given in Table 1. In this situation, due to the pulsating component, the time periodic flow field occurred in the channel, and heat transfer was periodically achieved. Therefore, the heat transfer calculations are carried out according to the amount of heat transfer achieved over a cycle. In other words the flow is assumed to be time periodic. To explain how the mechanisms behave over a cycle, phase angles have been used and are denoted by "ωt". The 2π radian indicates a cycle. The numerical evaluations are performed after the system achieved fully time periodic state. First, the geometry is fixed at $w/H = 0.75$ and $L/H = 6$ to understand the effect of other parameters. The two main parameters are amplitude (A_0) and frequency (Wo) affecting the heat transfer characteristics in the pulsating flow. To clearly understand the role that these parameters play in heat transfer, the velocity and temperature profiles over a cycle are obtained for different amplitudes while the frequencies remain constant. The temperature and velocity profiles for a constant frequency ($Wo \approx 20$) and different amplitudes with phase angle 180° are shown in Fig. 4(a) and 4(b), respectively. The temperature field is observed as propagating more quickly into the channel with increasing amplitude compared with the steady flow.

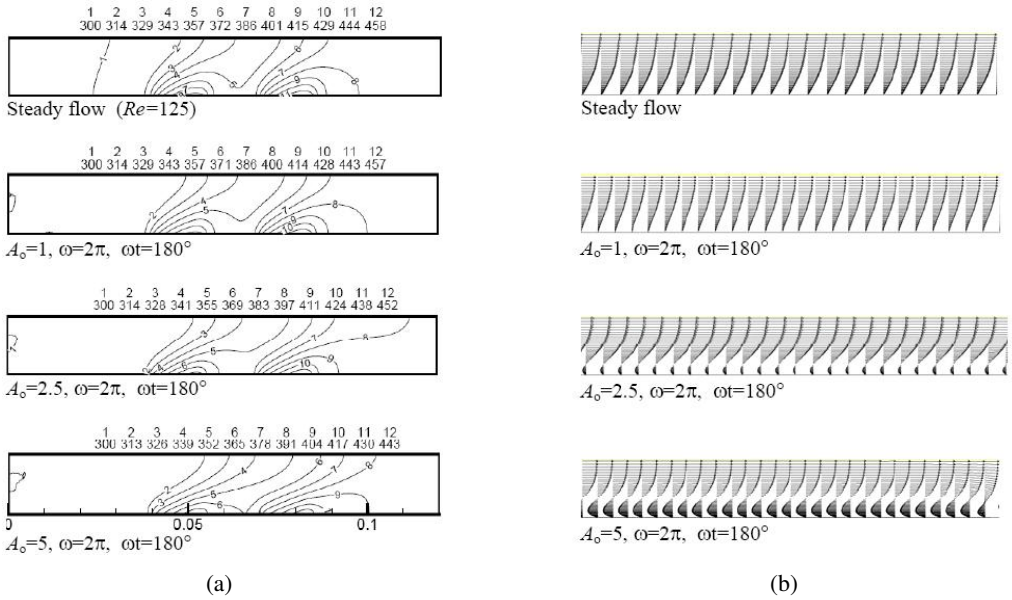

Fig. 4. (a) Temperature contours for different amplitude at fixed frequency and specific phase angle ($Wo \approx 20$, $w/H = 0.75$), (b) Velocity vectors for situations in Fig. 4(a), ($Wo \approx 20$, $w/H = 0.75$).

A comparison of velocity profiles between steady flow and pulsating flow conditions for the lowest amplitude specified by $A_0 = 1$ shows that they are approximately the same as each other, as seen in Fig. 4(b). This case showed no significant effects of low amplitudes on heat transfer enhancement. However, for $A_0 = 2.5$ and $A_0 = 5$, it is observed that due to the pulsating effect, the velocity profile is reversed at around the boundary layer for specific phase angles of the cycle, as seen in Fig. 4(b). These effects destroy the boundary layer form very fast and as a consequence, the heat transfer rate is increased. It means that for higher amplitude, the heat transfer rate is faster near the wall, and consequently, the temperature near the wall responds faster with regard to velocity variations.

The temperature contours over a cycle for a low frequency ($Wo = 14$), and high amplitude ($A_0 = 5$) are represented in Fig. 5(a). In a comparison of these contours with a steady flow (seen in Fig. 4a), the pulsating flow temperature contour is different and changed for each step of the cycle. In pulsating flow, because of the phase lag between boundary layer and core flow, a larger velocity gradient occurs at the boundary layer region, as seen in Fig. 5(b). Due to these effects, the thermal boundary layer is destroyed faster, and as a consequence the heat transfer is affected by this phenomenon [29]. So, the fluids within the boundary layer near the heaters are away from the wall. As seen in Fig. 5(a), the temperature profiles near the wall are destroyed, and the heat contained in the boundary layer is transferred into the core flow. For different phase angle, a new boundary layer is formed with fresh bulk fluid around the boundary region. Thus, this phenomenon provides an effective heat transfer rate from the heat source to the fresh boundary layer during each cycle. The variation of instantaneous wall temperature along the channel is illustrated for a frequency

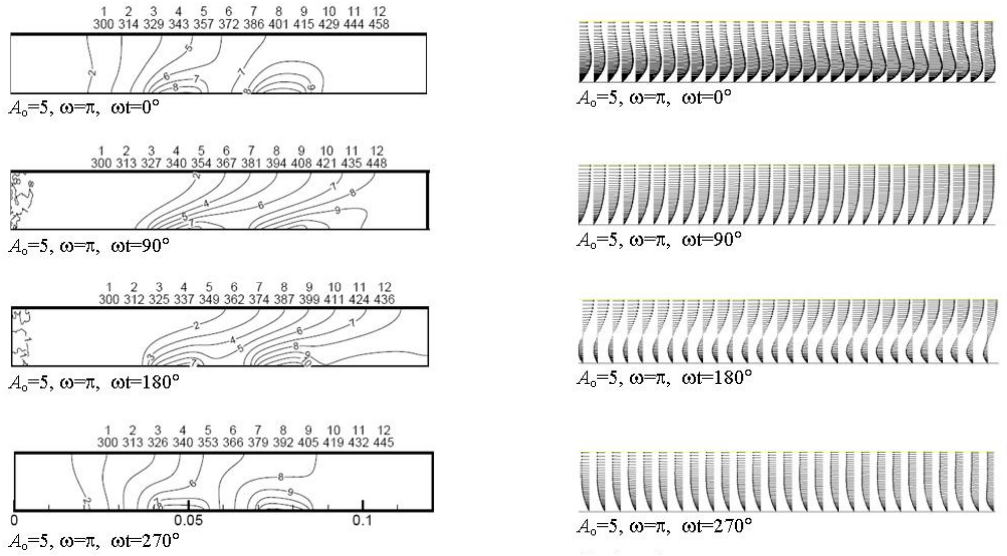

(a) (b)

Fig. 5. (a) Temperature contours for various phase angles over a cycle ($A_0 = 5$, $Wo \approx 14$, $w/H = 0.75$), (b) Velocity vectors for situations in Fig. 5(a), ($A_0 = 5$, $Wo \approx 14$, $w/H = 0.75$)

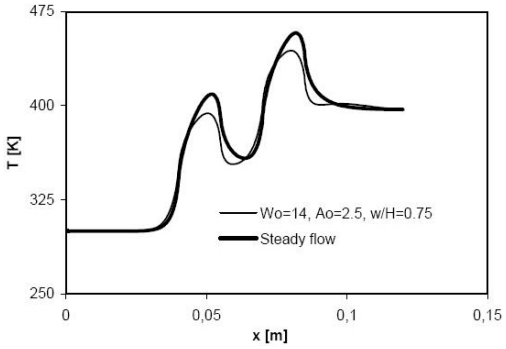

Fig. 6. The instantaneous temperatures along the wall for pulsating flow ($Wo = 14$, $A_0 = 2.5$, $w/H = 0.75$) and steady flow conditions.

($Wo = 14$) and an amplitude ($A_0 = 2.5$) in Fig. 6. From the figure it is evident that, due to dominance of conduction dissipation from the heaters, the two discrete heater surfaces have different kinds of temperature variation. Along the wall, the surface temperature raises at the beginning of each heater and slides down near the end of the heater. The variation is more near the second heater due to the thermal wake produced by the first heater. For comparison purposes, the temperature variation for steady flow at the wall boundary is given in the figure, which is higher than pulsatile flow wall temperature. It can be concluded that pulsating flow slightly increases the cooling performance of hot surfaces.

5.1. Calculation of Nusselt Numbers

To calculate the heat transfer for pulsating flow such as steady channel flow ($Nu_s = h_s H/k$), the local instantaneous Nusselt number along the heated wall can be expressed as follows:

$$Nu_{x,t} = \frac{h(x,t)H}{k}\,, \tag{8}$$

where k is thermal conductivity of the fluid and h is the local instantaneous heat transfer coefficient. The overall heat transfer coefficient is obtained by an integration of the local and instantaneous heat transfer coefficient over a cycle for each heater wall:

$$h_p = \frac{1}{\tau l}\int_0^{\tau}\int_0^{l} h(x,t)\,dx\,dt\,, \tag{9}$$

where τ is the time of the cycle, and l is the heater length. In this case, the time-averaged local Nusselt number is defined as:

$$Nu_t = \frac{1}{\tau}\int_0^{\tau} Nu_{x,t}\,dt\,. \tag{10}$$

The space-averaged local Nusselt number is defined as:

$$Nu_x = \frac{1}{l}\int_{x_1}^{x_2} Nu_{x,t}\,dx\,, \tag{11}$$

where x_1 is the beginning and x_2 is the end of the heater-1. For heater-2, a similar definition is used. On the other hand, the overall Nusselt number for pulsating flow can be defined by considering Eq. (9) with substitution into Eq. (8). The cycle average Nusselt number is defined as follow:

$$Nu_p = \frac{q''H}{k(\overline{T}_w - \overline{T}_b)}\,, \tag{12}$$

where $\overline{T}_w$ is the cycle average heater wall temperatures, and $\overline{T}_b$ is the cycle average fluid temperatures of the whole channel, which is obtained as an area-weighted average of nodal points at the solution domain, and expressed as follows:

$$\overline{T}_b = \frac{\int_A |u(y,t)|\,T(x,y,t)\,dA}{\int_A |u(y,t)|\,dA}\,. \tag{13}$$

The instantaneous Nusselt number over a cycle for heater-1 is depicted in Fig. 7, for three different amplitudes. The value of Nusselt number is found to be high at higher amplitude. The variation is approximately

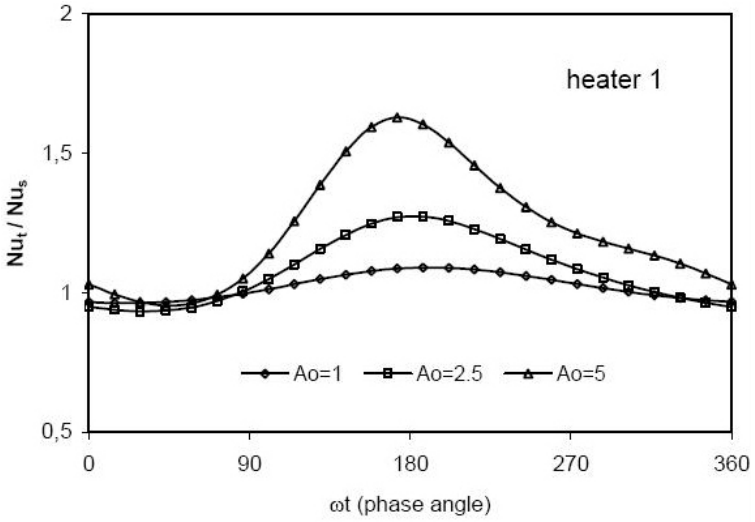

Fig. 7. Temporal variations of the instantaneous Nusselt number over a cycle ($Wo = 20$, $w/H = 0.75$).

sinusoidal, and the variation of Nusselt number at high amplitude is remarkable. However, there is a phase difference between hydrodynamic boundary layer near the wall and core flow, this is because the flow reversal at the higher amplitude. Also, it can be concluded that, there is phase difference between the axial velocity and temperature variations. As a consequence, the phase difference based on the pulsating flow would cause the asymmetric around (non-sinusoidal) for local Nusselt number at increasing amplitudes. Physically, a higher value of amplitude means a larger amount of fluid is heated by the heaters during each cycle. The temperature near the wall responds faster with respect to the velocity variation, and consequently, heat transfer rate is increased, as shown in the Fig. 7.

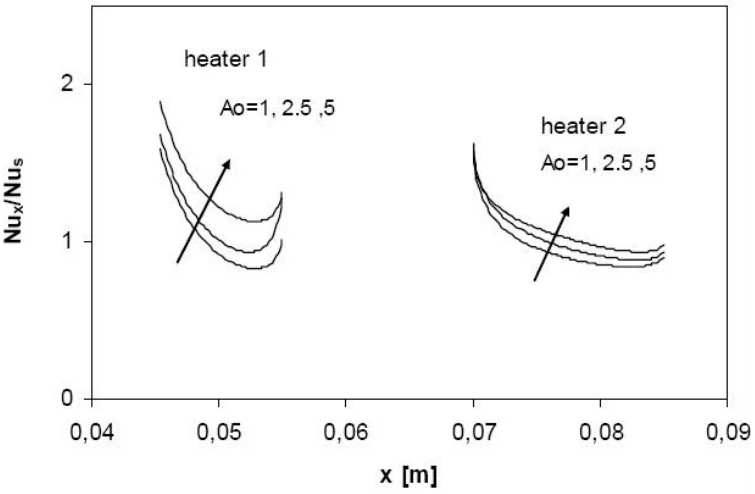

Fig. 8. Local Nusselt number along the discrete heaters ($Wo = 20$, $w/H = 0.75$).

The local Nusselt number along the discrete heaters is shown in Fig. 8, depending on the amplitudes for a specific frequency. The value of the local Nusselt number is found to be high at the beginning edge of each heater, irrespective of the position, with a decrease in the Nusselt number thereafter. It is also increased toward the end of the first heater. It can be concluded that, for a given Womersley number, the highest

heat transfer is found for higher amplitude and the first heater heat transfer rate is higher than that of the second heater for all cases. This phenomenon indicates the significant surface temperature gradient at the first heater. Due to the thermal wake effect, the heat transfer rate of the second heater is fairly low. In such a case, it should be evaluated as a geometric parameter to obtain the optimum heat transfer rate, which is analyzed in the last section.

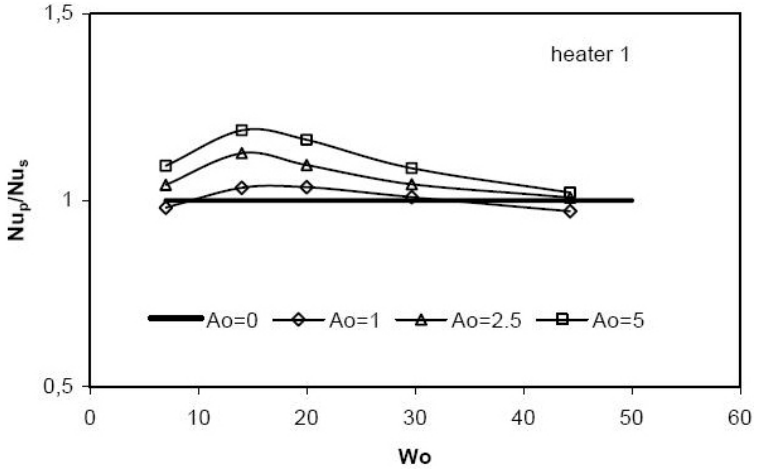

Fig. 9. Average Nusselt numbers versus dimensionless parameters for heater 1 ($w/H = 0.75$).

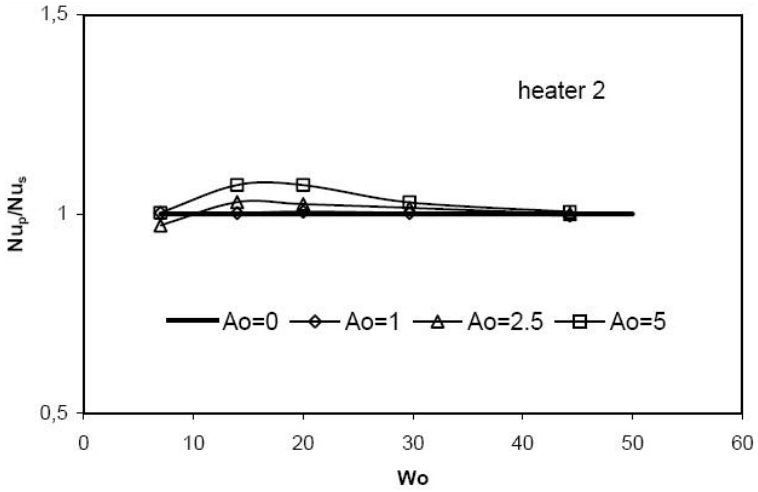

Fig. 10. Average Nusselt numbers versus dimensionless parameters for heater 2 ($w/H = 0.75$).

In this study, the calculated cycle average Nusselt number is given depending on dimensionless parameters, as seen in the Figs. 9 and 10 for heater-1 and heater-2, respectively. In these figures, the Nusselt number is shown as depending on the dimensionless Womersley number (Wo) and dimensionless amplitude A_0 where, $A_0 = 0$ shows steady flow conditions. Numerical calculations are performed, and the pulsating effect enhances heat transfer to a specific part of the dimensionless parameters compared with the steady flow heat transfer rate as shown in the figures. As shown in Figs. 9 and 10, the pulsating effect enhances the heat transfer at a low frequency and high amplitude. Although heat transfer is also increased at low amplitudes the increase is not remarkable compared with steady flow. However, the computed results reveal that the heat transfer characteristics go towards to the steady flow conditions while increasing the frequency

for any amplitude values. It was also concluded that the pulsating effect decreased the heat transfer rate at both low amplitude and low frequency as seen in the figures. In this case, as seen in Figs. 9 and 10, it can be concluded that optimum heat transfer enhancements are performed at low frequencies and high amplitudes.

This phenomenon can be explained by analyzing the structure of pulsating flow. At high amplitude values, the fluid in the boundary layer close to the heated wall is transferred toward the core flow with very high velocity, which increased the convective effect, and a warmer fluid is conveyed far away to the colder fluid region. Consequently, the temperature profile near the wall is destroyed, and the heat contained in the boundary layer is transferred into the core flow. Similarly, providing high performance at a low frequency can be expressed based on conveying the warmer fluid that has sufficient time to lose the heat contained in the flow. It is relevant to note that the increase in the heat transfer is more sensitive to amplitude than to frequency, because high amplitude increases the convective effect in the flow, and very high heat transfer is achieved by fluid displacements [30].

Due to the potentially large number of geometric parameters, a limited parameter is changed. First of all, a geometry fixed at $w/H = 0.75$ and other main parameters are investigated. In the second part of this study, we continued with changed limited geometric parameters due to the computational cost. For this situation, the pulsating parameters are fixed at $A_0 = 5$ and at $Wo = 14$. The geometric parameter effect is expressed by the ratio of spacing between two heaters and the channel height as w/H. Where, the distances from the channel entrance to the first heater, and the distance from the second heater to the channel exit, are not changed. Only, the distance between two heaters is changed. The effect of heater location on the temperature distribution and velocity vectors in a specific phase angle ($\omega t = 210°$) for four different locations of heaters ($w/H = 0.375,\ 0.75,\ 1.15,\ 1.5$) is illustrated in Fig. 11(ab).

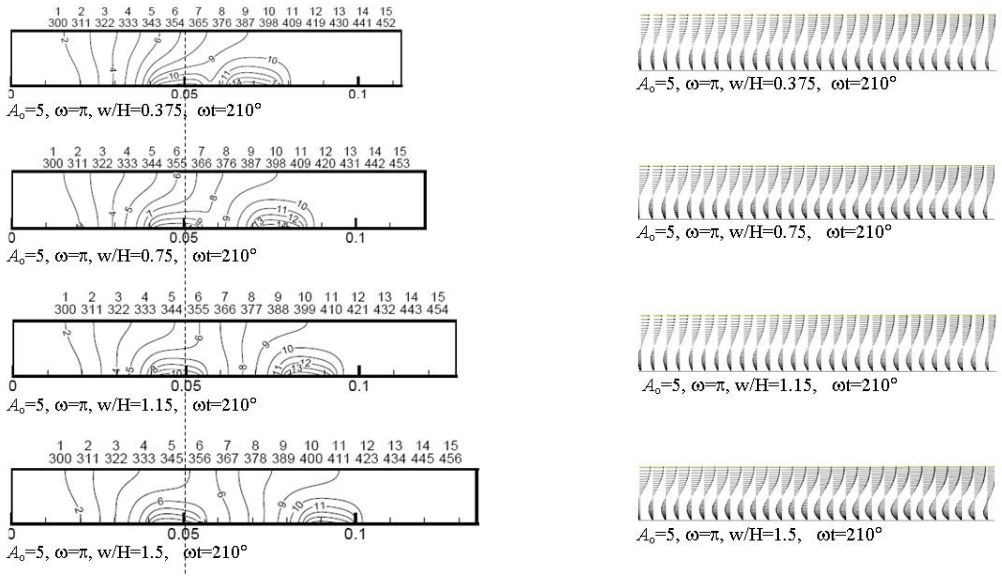

Fig. 11. (a) Temperature contours for different w/H at fixed frequency and specific phase angle ($Wo \approx 14$), (b) Velocity vectors for situations in Fig. 11(a) ($Wo \approx 14$).

The results are similar to previously studied cases for velocity, while the temperature distributions changing depend on the heater locations. The temperature contours are sharply peaked into the core flow in the fluid across the channel. The wake effect of the thermal boundary layer decreases with the increasing of the

w/H range. The average Nusselt numbers calculated for four different ranges of w/H are given in Fig. 12. It is found that the ratio w/H has a remarkable effect on the average Nusselt numbers.

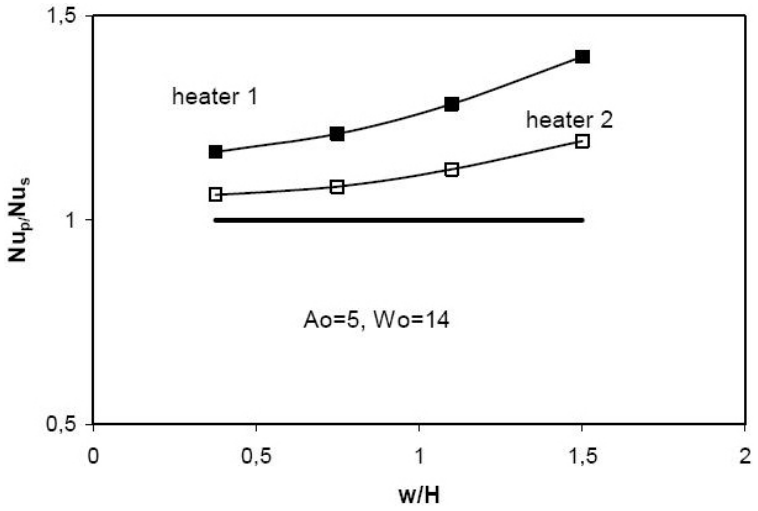

Fig. 12. The effect of distance between two heaters on the average Nusselt Numbers ($A_0 = 5$, $Wo = 14$).

As shown in Fig. 12, the heat transfer rate is a noticeable increase with increasing the distance between two heaters. The increasing in heater-2 is a little lower than the heater-1. There is always a wake effect in any event for the sequentially location of heaters. However, a higher Nu number is obtained for the second heater, if the distance between heaters continues to increase and has reaches the independence of each other [31,32].

6. CONCLUSIONS

In this study, a laminar unsteady convective heat transfer around two discrete heaters in a channel subjected to pulsating flow of air is numerically investigated using Fluent CFD package. The flow and energy equations are solved for a fixed Reynolds number ($Re = 125$). Investigations are performed for five different frequencies and three amplitudes. In addition, limited geometric parameters; the distance between the heaters are investigated. In the first part of the study, the problem geometry is fixed at $w/H = 0.75$. Then, the amplitude (A_0) and frequency (Wo) effect for the heat transfer enhancements is considered. Flow parameters such as the Nusselt numbers are obtained based on the time mean average over a cycle and compared with the available literature to verify the code findings. The velocity profiles and temperature isotherms were obtained to understand and interpret the flow and heat transport. It was observed that with high fluid amplitude and low Womersley numbers, there is an increased heat transfer rate. It should be noted that the heat transfer enhancement was about 35 % for a high amplitude ($A_0 = 5$) and a low frequency ($Wo = 14$), compared with the steady flow under similar conditions. However, increasing the frequency over a specific value causes a negative effect on the heat transfer. In the second part of study, the amplitude and frequency are fixed ($A_0 = 5$, $Wo = 14$), and the spacing between heaters are changed in the range of $0.375 < w/H < 1.5$. The heat transfer rate is increased noticeably with the increase of the distance between heaters. The computed results reveal that the maximum heat transfer takes place at the first heater as expected. Due to the thermal wake effect of the first heater, the heat transfer from the second heater is fairly low according to the first one. Based on the results obtained in the present simulations, the effect of other physical parameters should be investigating future numerical works.

REFERENCES

1. Tseng, Y.-S., Fu, H.-H., Hung, T.-C. and Pei, B.-S., "An optimal parametric design to improve chip cooling", *Applied Thermal Engineering*, Vol. 27, Nos. 11–12, pp. 1823–1831, 2007.
2. Lasance, C.J.M. and Simons, R.E., "Advances in high performance cooling for electronics", *Electronics Cooling*, Vol. 11, No. 4, pp. 22–39, 2005.
3. Yeh, L.T., "Review of heat transfer technologies in electronic equipment", *ASME Journal of Electronic Packaging*, Vol. 117, No. 4, pp. 333–339, 1995.
4. Bejan, A. and Ledezma, G.A, "Thermodynamic optimization of cooling techniques for electronic packages", *International Journal of Heat Mass and Transfer*, Vol. 39, No. 6, pp. 1213–1221, 1996.
5. Carpinlioglu M. and Gundogdu, M.Y., "A critical review on pulsatile pipe flow studies directing towards future research topics", *Flow Measurement and Instrumentation*, Vol. 12, No. 3, pp. 163–174, 2001.
6. Carpinlioglu, M., "An approach for transition correlation of laminar pulsatile pipe flows via frictional field characteristics", *Flow Measurement and Instrumentation*, Vol. 14, No. 6, pp. 233–242, 2003.
7. Zamir, M., *The Physics of Pulsatile Flow*, Springer, New York, USA, 2000.
8. Havemann H.A., Rao, N.N., "Heat transfer in pulsating flow", *Nature*, Vol. 7, No. 41, p. 4418, 1954.
9. Habib M.A., Attya A.M., Eid A.I. and Aly A.Z., "Convective heat transfer characteristics of laminar pulsating pipe air flow", *Heat and Mass Transfer*, Vol. 38, No. 3, pp. 221–232, 2002.
10. Al-Haddad, A. and Al-Binally, N., "Prediction of heat transfer coefficient in pulsating flow", *International Journal of Heat and Fluid Flow*, Vol. 10, No. 2, pp. 131–133. 1989.
11. Ishino, Y., Suzuki, M., Abe,T., Ohiawa, N. and Yamaguchi, S., "Flow and heat transfer characteristics in pulsating pipe flow", *Heat Transfer-Japanese Research*, Vol. 25, No. 5, pp. 323–341, 1996.
12. Zheng, J., Zeng, D., Wang, P. and Gao, H., "An experimental study of heat transfer enhancement with pulsating flow", *Heat Transfer-Asian Research*, Vol. 23, No. 5, pp. 279–286, 2004.
13. Kearney, S.P., Jacobi, A.M. and Lucht, R.P., "Time-resolved thermal boundary layer structure in a pulsatile reversing channel flow", *ASME Journal of Heat Transfer*, Vol. 123, No. 4, pp. 655–664. 2001.
14. Mostafa, H. M., Torki, A.M. and Abd-Elsalam, K. M., "Experimental study for forced convection heat transfer of pulsating flow inside horizontal tube", *4th International Conference on Heat Transfer, Fluid Mechanics and Thermodynamics*, Cairo, Egypt, paper no. AK3, 2005.
15. Zohir, A.E., Habib, M.A., Attya A.M. and Eid, A.I., "An experimental investigation of heat transfer to pulsating pipe air flow with different amplitudes", *Heat and Mass Transfer*, Vol. 42, No. 7, pp. 625–635, 2006.
16. Mamayev, V.V., Nosov, V.S. and Syromyatnikov N.I., "Investigation of heat transfer in pulsed flow of air in pipes", *Heat Transfer-Soviet Research*, Vol. 8, No. 3, pp. 111–116, 1976.
17. Siegel R.and Perlmutter M., "Heat transfer for pulsating laminar duct flow", *ASME Journal of Heat Transfer*, Vol. 84, No. 2, pp. 111–122, 1962.
18. Faghri, M., Javadani, K. and Faghri, A., "Heat transfer with laminar pulsating flow in a pipe", *Letters in Heat and Mass Transfer*, Vol. 6, No. 4, pp. 259–270, 1979.
19. Moschandreou T. and Zamir M., "Heat transfer in a tube with pulsating flow and constant heat flux", *International Journal of Heat and Mass Transfer*, Vol. 40, No. 10, pp. 2461–2466, 1997.
20. Guo Z. and Sung H.J., "Analysis of the Nusselt number in pulsating pipe flow", *International Journal of Heat and Mass Transfer*, Vol. 40, No. 10, pp. 2486–2489, 1997.
21. Hemida H.N., Sabry M.N., Abdel-Rahim A. and Mansour H., "Theoretical analysis of heat transfer in laminar pulsating flow", *International Journal of Heat and Mass Transfer*, Vol. 45, No. 8, pp. 1767–1780, 2002.
22. Yu J.C., Li Z. and Zhao T.S., "An analytical study of pulsatile laminar heat convection in a circular tube with constant heat flux", *International Journal of Heat and Mass Transfer*, Vol. 47, pp. 5297–5301, 2004.
23. Nield D.A. and Kuznetsov, A.V., "Forced convection with laminar pulsating flow in a channel or tube", *International Journal of Thermal Sciences*, Vol. 46, No. 6, pp. 551–560, 2007.
24. Cho H.W. and Hyun J.M., "Numerical solution of pulsating flow and heat transfer characteristics in a pipe", *International Journal of Heat and Fluid Flow*, Vol. 11, No. 4, pp. 321–330, 1990.
25. Chang Y.M. and Tucker P.G., "Numerical studies of heat transfer enhancements in laminar separated flows", *International Journal of Heat and Fluid Flow*, Vol. 25, No. 1, pp. 22–31, 2004.

26. Mostafa, H. M., Abd-Elsalam, K. M. and Torki, A.M., "Theoretical study of laminar pulsating flow in a pipe", *International Conference on Thermal Issues in Emerging Technologies: Theory and Application, THETA 2007*, pp. 219–224, Cairo, Egypt, January 3–6th, 2007.
27. Chattopadhyay, H., Durst, F. and Ray, S., "Analysis of heat transfer in simultaneously developing pulsating laminar flow in a pipe with constant wall temperature", *International Communications in Heat and Mass Transfer*, Vol. 33, No. 4, pp. 475–481, 2006.
28. Kim S.Y., Kang B.H. and Hyun J.M., "Heat transfer in the thermally developing region of a pulsating channel flow", *International Journal of Heat and Mass Transfer*, Vol. 36, No. 17, pp. 4257–4266, 1993.
29. Zhao, T.S. and Cheng, P. A., "Numerical solution of laminar forced convection in a heated pipe subjected to a reciprocating flow", *International Journal of Heat and Mass Transfer*, Vol. 38, No. 16, pp. 3011–3022, 1995.
30. Akdag, U., "Numerical investigation of pulsating flow around a discrete heater in a channel", *International Communications in Heat and Mass Transfer*, Vol. 37, No. 7, pp. 881–889, 2010.
31. Bhowmik, H., Tso, C. P. and Tou, K. W., "Analyses of convection heat transfer from discrete Heat sources in a vertical rectangular channel", *Journal of Electronic Packaging*, Vol. 127, No. 3, pp. 215–222, 2005.
32. da Silva, A.K. Lorente, S. and Bejan, A., "Optimal distribution of discrete heat sources on a plate with laminar forced convection", *International Journal of Heat and Mass Transfer*, Vol. 47, Nos. 10–11, pp. 2139–2148, 2004.
33. Incropera F.P., Kerby J.S., Moffatt D.F. and Ramadhyani, S., "Convection heat transfer from discrete heat sources in a rectangular channel", *International Journal of Heat and Mass Transfer*, Vol. 29, No. 7, pp. 1051–1058, 1986.
34. McEntire, A.B. and Webb, B.W., "Local forced convective heat transfer from protruding and flush-mounted two-dimensional discrete heat sources", *International Journal of Heat and Mass Transfer*, Vol. 33, No. 7, pp. 1521–1533, 1990.
35. Tso, C.P., Xu, G.P. and Tou, K.W., "An experimental study on forced convection heat transfer from flush-mounted discrete heat sources", *ASME Journal of Heat Transfer*, Vol. 121, No. 2, pp. 326–332, 1999.
36. Chen, S. Liu, Y., Chan, S.F., Leung, C.W. and Chan, T.L., "Experimental study of optimum spacing problem in the cooling of simulated electronics package", *Heat and Mass Transfer*, Vol. 37, Nos. 2–3, pp. 251–257, 2001.
37. Wang, C.Y., "Optimum placement of heat-sources in forced convection", *ASME Journal of Heat Transfer*, Vol. 114, No. 2, pp. 508–510, 1992.
38. Atabek, H.B. Chang C.C. and Fingerson L.M., "Measurement of laminar oscillatory flow in the inlet length of a circular tube", *Physics in Medicine and Biology,* Vol. 9, No. 2, pp. 219–227, 1964.
39. Incropera, F. and Dewitt, P.D., *Fundamentals of Heat and Mass Transfer*, 3rd Edition, John Wiley & Sons Inc., New York, USA, 1996.